Air Distribution in Rooms, (ROOMVENT 2000)
Editor: H.B. Awbi

ZONAL MODELS USING LOOP EQUATIONS AND SURFACE DRAG CELL-TO-CELL FLOW RELATIONS

James W. Axley

School of Architecture, Yale University
New Haven, CT 06520, USA

ABSTRACT

Zonal models have been proposed to bridge the gap between the whole-building macroscopic modeling methods of programs like CONTAM or COMIS and the more detailed microscopic modeling methods based on solutions of the time-smoothed Navier-Stokes equations for room airflows. This paper identifies a critical shortcoming of conventional approaches to zonal modeling by introducing alternative approaches a) to formulate the key cell-to-cell flow relations upon which zonal models are based and b) to assemble the zonal system equations. Conventional cell-to-cell flow relations based on boundary power-law formulations appear to capture gross aspects of the flow structure in rooms but fail by orders of magnitude to properly model the resistance offered to airflow. Cell-to-cell flow models based on surface drag momentum transfer may mitigate this shortcoming and appear to capture room airflow structure more accurately. Furthermore, these flow models offer a means to provide quick approximate solutions of room airflow problems (i.e., based on linear formulations of cell-to-cell flow relations) that may be acceptable for certain purposes or can be used as initial estimates for the solution of the more accurate nonlinear formulations of zonal problems.

KEYWORDS

Air Flow, Air Distribution, Modeling, Network Models, Zonal Models, Loop Equations, CONTAM

INTRODUCTION

A number of innovative mechanical and natural ventilation, cooling and heating strategies put forward in recent years depend critically on the details of airflow within rooms and their variation with time. Whole building macroscopic models, such as the CONTAM and COMIS models (Pelletret and Keilholz 1997; Walton 1997), have been developed to predict time histories of bulk airflows into, out of and between rooms in building systems but ignore the details of room airflows altogether. Microscopic models, on the other hand, provide this detail but can not yet be applied to studies of complex whole building systems, are often limited to steady conditions, and demand personnel and computational resources well beyond that of current macroscopic modeling tools. Consequently, a number of proposals have been offered to extend available macroscopic models to provide at least an approximate evaluation of the details of room airflows for whole building annual simulation studies.

These *zonal models* have quite logically been formulated by subdividing rooms into a relatively small number of discrete control volumes or *cells*, formulating heat and mass transfer relations that approximate exchanges between these cells, and assembling these relations into system equations using fundamental conservation principles. In the Systems Dynamics literature such formulations are identified, generically, as *continuity laws* and are often contrasted to the alternative *compatibility laws* that may be used to formulate macroscopic system equations (Shearer, Murphy et al. 1971). In the zonal modeling context a *compatibility* approach would use a similar subdivision of a room into cells but would assemble system equations based on so-called *path laws* or *loop equations*.

The *compatibility* approach to zonal modeling has, apparently, been largely ignored. This paper will explore this alternative approach. In addition, the formulation of the key mass transfer relations that describe cell-to-cell airflow rates in existing zonal models will be critically reviewed and an alternative approach based on momentum transfer to surrounding walls will be presented. Comparisons to existing zonal models will be made and simple applications of these alternative methods explored.

THEORY

The general approach to zonal modeling employed here follows what has become common practice in the field (Allard 1998; Wurtz, Nataf et al. 1999). A room is subdivided into a number of control volumes or *cells*; temperature and pressure fields within the room, $T(x,y,z)$ and $p(x,y,z)$, are approximated by discrete values, T_i and p_i, associated with nodes located within each cell; and system equations are formulated that relate the cell-to-cell air mass flow rate, $\dot{m}_{i,j}$, with these approximate state variables, Figure 1a. This common zonal model is analogous to a resistance network laid out on an orthogonal grid or *mesh*, Figure 1b, with node voltages V_i and currents $i_{i,j}$ corresponding to node pressures p_i and air mass flow rates $\dot{m}_{i,j}$.

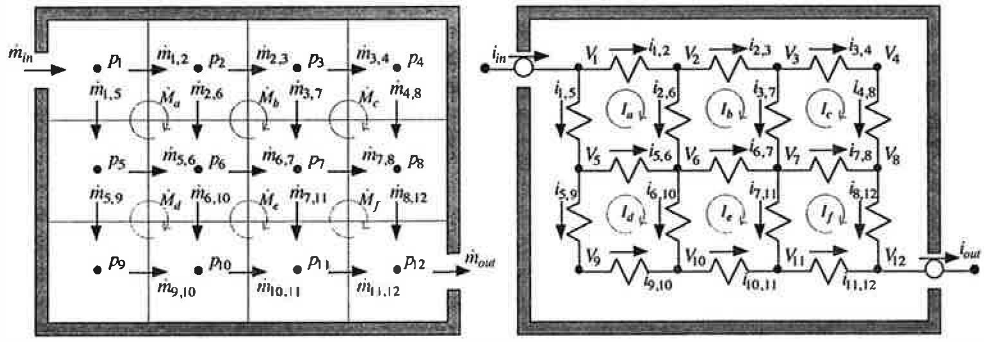

a) Typical Zonal Model b) Analogous Resistance Network

Figure 1 A multi-cell room model and analogous electrical resistance network.

Here, within each cell, temperatures are assumed to be uniform and equal to the cell discrete value T_i and pressures are assumed to vary hydrostatically about the cell discrete value p_i as:

$$T(x,y,z)\big|_{cell\ i} \cong T_i \quad , \quad p(x,y,z)\big|_{cell\ i} \cong p_i - \rho_i\, g\, z_i \qquad (1, 2)$$

where x and y are taken as horizontal coordinates, z is the vertical coordinate, z_i is the local elevation relative to the cell node, and ρ_i is the uniform air density within the cell.

System equations may then be formulated using one of two fundamental principles – *continuity* of flow at each node (i.e., mass or energy conservation in the zonal model or current continuity in the resistance network), or *compatibility* of state variable changes as one traverses any path around a continuous *loop* in the model:

$$\textit{Continuity} \qquad \sum_k \dot{m}_{k,j} - \sum_l \dot{m}_{j,l} = 0 \;\; ; \;\; \left\{ \sum_k i_{k,j} - \sum_l i_{j,l} = 0 \right\} \tag{3}$$

$$\textit{Compatibility} \qquad \sum_{i,j} \left(p_i - p_j \right) = 0 \;\; ; \;\; \left\{ \sum_{i,j} \left(V_i - V_j \right) = 0 \right\} \tag{4}$$

where k and l are permuted through the indices of all adjacent cells (i.e., up to six cells in the 3D case) and i,j in Equation 4 are permuted through the indices around a given loop.

System Equations: Commonly, the continuity approach has been applied in zonal modeling by formulation of *inverse* expressions that relate the cell-to-cell air mass flow rates to the linked state variables as:

$$\textit{Inverse Flow Expression:}\; m_{i,j} = g\left(p_i, T_i, p_j, T_j\right) \;\; ; \;\; \left\{ i_{i,j} = \Delta V_{i,j} / R_{i,j} \right\} \tag{5}$$

System equations are then assembled by systematically applying the continuity equation (Equation 3) to each node using Equation 5 or semi-empirical expressions for known jets or plumes in the room. Coupled systems of nonlinear equations are thus obtained that may be solved to determine the cell state variables p_i and T_i. Unknown air mass flow rates are then recovered using Equation 5.

Alternatively, *forward* expressions may be formed that relate pressure changes to air mass flow rates and node temperatures as (with $\Delta p_{i,j} = p_i - p_j$):

$$\textit{Forward Flow Expressions:}\; \Delta p_{i,j} = f\left(m_{i,j}, T_i, T_j\right) \;\; ; \;\; \left\{ \Delta V_{i,j} = i_{i,j} R_{i,j} \right\} \tag{6}$$

In this approach system equations are then assembled by systematically applying the compatibility equation (Equation 4) to each of a set of *independent* loops and complementing this set of equations with the node continuity equation (Equation 3) applied at *(n-1)* of the *n* nodes of the zonal model. Graph theory reveals that the simple *mesh loops* linking four adjacent nodes (e.g., the directed loops with hypothetical flow rates $\dot{M}_a$, $\dot{M}_b$, … in Figure 1a or analogously I_a, I_b, … in Figure 1b) yield an independent set of loop equations (Shearer, Murphy et al. 1971). Furthermore, for linear forward flow expressions the system equations may be defined in terms of these hypothetical mesh loop flow rates to minimize the number of system equations. The influence of known room jets or plumes is, in this case, used to constrain individual loop equations.

Cell-to-Cell Mass Flow Expressions: Inverse flow expressions have been based on methods used for large openings. In this approach flow resistance is assumed to occur at the boundary between cells, Figure 2a, and a power-law relation is assumed to govern the differential mass flow $d\dot{m}_{i,j}$ through differential areas of the boundary dA as:

$$d\dot{m}_{i,j} = C\rho\left(\Delta P_{i,j}\right)^n dA \tag{7}$$

C is an empirical "permeability" constant, analogous to the orifice discharge coefficient, that is assumed to have a value less than 1.0 with one recent study concluding a value of 0.83 $m \cdot s^{-1} \cdot Pa^{-n}$ being most reliable (Wurtz, Nataf et al. 1999). The power-law exponent n is often taken as $n = 1/2$ which corresponds to the orifice equation and the air density ρ taken as the average of adjacent cells. Finally, the driving pressure difference $\Delta P_{i,j}$ follows directly from Equation 2 above:

$$\Delta P_{i,j} = \left(p_i - \rho_i g z_i\right) - \left(p_j - \rho_j g z_j\right) \tag{8}$$

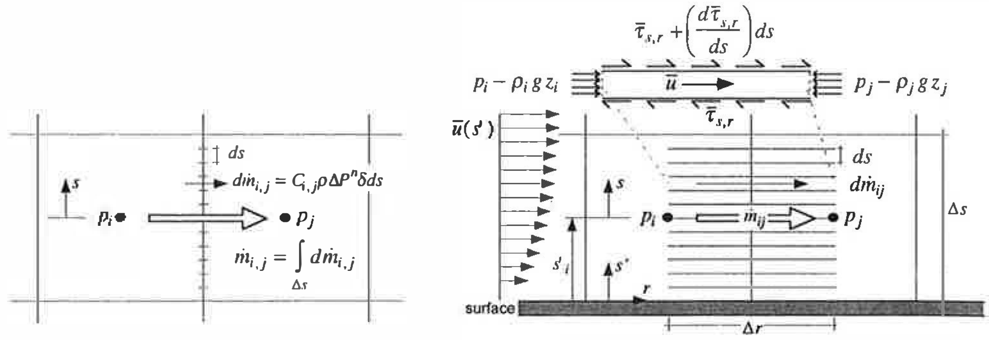

a) Cell Boundary Power-Law Flow Model b) Surface-Drag Momentum Balance Flow Model

Figure 2 Conventional a) and proposed b) cell-to-cell flow idealizations.

Expressions for the cell-to-cell air mass flow rate $\dot{m}_{i,j}$ may then be derived by integrating Equation 7 over the cell boundary area. For isothermal flow in a 2D flow regime of arbitrary depth δ one obtains:

$$\dot{m}_{i,j} = \int d\dot{m}_{i,j} = \int_{-\Delta s/2}^{\Delta s/2} C\rho\left(\Delta P_{i,j}\right)^{n} \delta\, ds = C\rho\delta\,\Delta s\left(\Delta P_{i,j}\right)^{n} \quad (9)$$

This model implicitly assumes viscous dissipation occurs only at the boundary – a reasonable approximation for an orifice but not room airflows dominated by surface drag. Thus when applied to airflow through a room, the total pressure drop will depend linearly on the number of cells used – clearly not a reasonable outcome. Furthermore, when recast in forward form and used to form loop equations, the flow solution proves to be independent of the permeability coefficient *C*!

An alternative approach may be developed by considering the transfer of shear stress near wall surfaces using a momentum balance on differential flow conduits linking adjacent cells, Figure 3b. For a flow conduit oriented parallel to the nearest room surface, pressures integrated over the ends of the conduit must balance (time-smoothed) shear stresses $\bar{\tau}_{sr}$ acting over the length of the conduit:

$$\Delta P_{i,j}\,\delta\, ds' = -\frac{d\bar{\tau}_{sr}}{ds'}\,\delta\,\Delta r\, ds' \quad (10)$$

where s' and r' are local normal and tangential coordinates to the surface and Δr is the cell width parallel to the surface. The shear stress may be related to the (time-smoothed) velocity profile perpendicular to the wall $\bar{u}(s')$ using the fundamental relation for Newtonian fluids for laminar flow and, here, Prandtl's mixing length relation for turbulent flow that has proven to be effective in CFD simulations of room air flow (Chen and Xu 1998):

$$\textit{Laminar Flow: } \bar{\tau}_{sr} = -\mu\frac{d\bar{u}}{ds'} \quad , \quad \textit{Turbulent Flow: } \bar{\tau}_{sr} = -\rho\kappa^{2}s'^{2}\left(\frac{d\bar{u}}{ds'}\right)^{2} \quad (11, 12)$$

where κ is a "universal constant" with empirically determined values ranging from 0.36 to 0.40.

To effect closure, relations for the velocity profiles are needed – for this empirical equations of the following form for laminar and turbulent flow respectively may be used:

$$\textit{Laminar Flow: } \bar{u} = \bar{u}_{\max}\sin(\pi s'/2S) \quad , \quad \textit{Turbulent Flow: } \bar{u} \approx \bar{u}_{\max}(s'/S)^{a} \quad (13, 14)$$

where $\bar{u}_{\max}$ is a hypothetical asymptotic maximum approached as $s' \to S$, S is a characteristic room dimension taken as half the dimension between opposing room walls, and a is an empirically determined coefficient. Well-developed turbulent velocity profiles in tubes and ducts are well approximated with $a = 1/7$ – the value that will be used in subsequent applications.

Finally, flow relations may be derived by substituting these expressions into the momentum balance, Equation 10, and integrating over the cell height Δs. For isothermal conditions one obtains:

$$\text{2D Laminar: } \Delta P_{i,j} = \frac{\mu \pi^2 \Delta r}{4 \rho S^2 \delta \Delta s} \dot{m}_{i,j} \quad , \quad \text{2D Turbulent: } \Delta P_{i,j} = 2k_s \frac{\kappa^2 a^3 \Delta r}{\rho \delta^2 \Delta s^3} \dot{m}_{i,j}^{\,2} \qquad (15, 16)$$

Here, k_s is defined uniquely for each cell position $n_s = 1,2,3,\ldots$ relative to the nearest surface with $k_s \approx 4/(4n_s - 3)$ for central cells of odd meshes or $k_s \approx 2/(2n_s - 1)$ for all other cells. The extension of this cell-to-cell airflow model to 3D flow regimes and nonisothermal conditions is straightforward. Details are available from the author and will be presented in other publications.

APPLICATIONS

Isothermal applications of zonal models should reasonably be used for validation before consideration of more challenging nonisothermal cases are considered. Two cases are considered below.

Duct Flow Modeling: The 3D variants of both the laminar and turbulent surface drag cell-to-cell flow models, Equations 15 and 16, and the power-law boundary flow model, Equation 9, with n=1/2 were applied to the problem of modeling airflow through a 6m length of a square duct 2m x 2m. Four turbulent surface-drag idealizations were considered utilizing 1x1, 2x2, 3x3, and 4x4 cell subdivisions across the section and 4 cell subdivisions along the length of the duct. These were compared to 1x1x4 cell subdivisions of both the laminar surface-drag model and the conventional power-law model as cross-sectional subdivision has no impact on the results using these flow models for this particular flow problem.

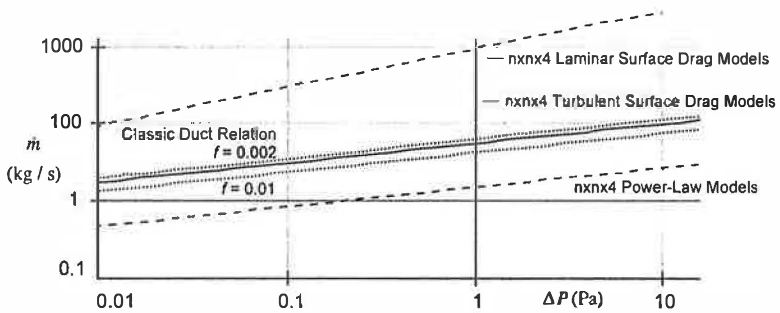

Figure 3 Comparison of modeled duct pressure-flow relations for the surface drag and power-law flow models and the classic Darcy-Weisbach equation for friction factors from $f = 0.01$ to 0.002.

The turbulent surface drag idealizations produced duct pressure-flow relations essentially identical in form to the classic Darcy-Weisbach equation, adapted to rectangular cross-sections via the hydraulic radius approximation, with effective duct friction factors of $f_{eff} = 0.0034$, 0.0034, 0.0038, and 0.0040 for the 1x1, 2x2, 3x3, and 4x4 cross-sectional subdivisions respectively, Figure 3. Likewise the laminar surface drag idealization yielded duct pressure flow relations essentially identical in form to the classic Hagen-Poiseuille solution for the laminar case. Given the appearance of the cell-subdivision length Δr in both of these surface drag models, these idealizations yielded results that were independent of the number of longitudinal cell subdivisions used. Furthermore, the turbulent surface drag idealizations provided reasonable approximations to the velocity profiles across the duct that improved with cross-sectional subdivision.

The power-law idealization, on the other hand, yields pressure-flow relations that depend on the number of longitudinal cells used and does not provide any approximation of the velocity profile. For the 4-cell subdivision considered the resulting pressure-flow relation exhibited significantly greater resistance (i.e., by greater than an order of magnitude) for turbulent flow than the classic solution.

2D Forced Convection: The proposed surface drag and conventional power-law models were combined with well-established semi-empirical wall jet relations (Rajaratnam 1976) to model a 2D forced convection case studied by Chen (Chen and Xu 1998). Computed mass flow rates are shown below in Figure 4 for all idealizations. In this particular problem air is injected at the ceiling at a mass flow rate of 90 g/s (Re = 5,000) and is exhausted at the opposite floor.

Computed results are ordered by model as: (turb. surface drag, boundary power-law, lam. surface drag).

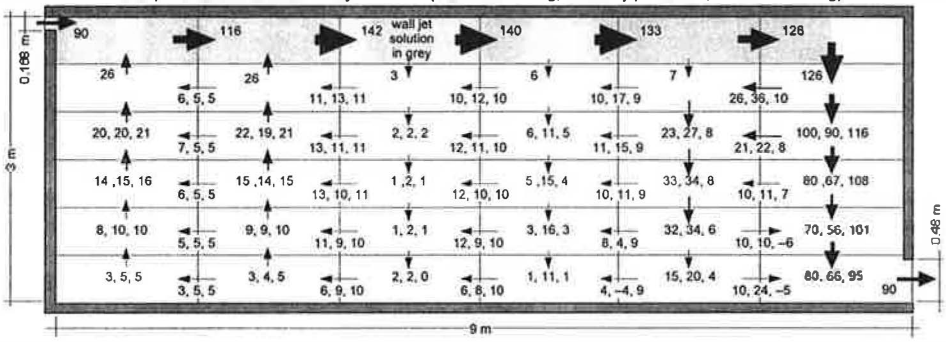

Figure 4 Comparison of computed results for a 2D forced convection problem.

Broadly speaking all cell-to-cell flow models provide similar results that compare reasonably well with the measured data and CFD computed results reported by Chen, although the turbulent surface drag model captures the nature of the flow intensification at the right wall more faithfully. Again, the power-law flow model resulted in a pressure drop from inlet to outlet that was over two orders of magnitude greater than that produced by the turbulent surface drag model. The success of the laminar surface drag model is perhaps most significant as this model produces linear system of algebraic equations, by either the continuity or compatibility approach, that may be easily solved. Furthermore, a very compact compatibility (loop) formulation of the system equations is possible using the hypothetical *mesh loop* flow rates discussed above. For quick approximate analysis the (linear) laminar surface drag solution may be acceptable. Alternatively, it may be used as a starting point for the solution of the much more difficult nonlinear analyses resulting from the use of the other models.

REFERENCES

Allard, F., Ed. (1998). Natural Ventilation in Buildings: A Design Handbook. London, James & James

Chen, Q. and W. Xu (1998). "A Zero-Equation Turbulence Model for Indoor Air Simulation." Energy and Buildings **Vol. 28**: pp. 137-144.

Pelletret, R. Y. and W. P. Keilholz (1997). COMIS 3.0 - A New Simulation Environment for Multizone Air Flow and Pollutant Transport Modeling. Building Simulation '97 - Fifth International IBPSA Conference, Prague, IBPSA.

Rajaratnam, N. (1976). Turbulent Jets. Amsterdam, Oxford, New York, Elsevier Scientific Pub. Co.

Shearer, J. L., A. T. Murphy, et al. (1971). Introduction to System Dynamics. Reading, MA, Addison-Wesley Pub. Co.

Walton, G. (1997). CONTAM96 User Manual. Gaithersburg, MD, NIST.

Wurtz, E., J.-M. Nataf, et al. (1999). "Two- and Three-dimenaional Natural and Mixed Convection Simulation using Modular Zonal Models in Buildings." International Journal of Heat and Mass Transfer(42): pp. 923-940.